Available online at www.sciencedirect.com
SCIENCE DIRECT
Journal of Catalysis 234 (2005) 356–363
JOURNAL OF CATALYSIS
www.elsevier.com/locate/jcat

Nanofibers of polyethylene produced by SBA-15 supported zirconium catalyst [N-(3-*tert*-butylsalicylidene)-4′-allyloxylanilinato]$_2$Zr(IV)Cl$_2$

Chao Guo, Dao Zhang, Fusong Wang, Guo-Xin Jin *

Laboratory of Molecular Catalysis and Innovative Material, Department of Chemistry, University of Fudan, Shanghai, 200433, China

Received 30 January 2005; revised 18 April 2005; accepted 5 June 2005

Available online 10 August 2005

Abstract

Ethylene polymerization was carried out with the zirconium catalyst bis[N-(3-*tert*-buttylsalicylidene)-4′-allyloxylanilinato] zirconium(IV) dichloride supported on SBA-15, which had a uniform hexagonal array of linear channels, with MAO (methylalumoxane) as the cocatalyst. Both the molecular weight and melting point of the obtained polymers were much higher, compared with the polyethylene produced by its homogeneous counterpart. This observation indicates that the mesoporous zeolite SBA-15 can effectively control the direction and dimension of the growth of polymers in the process of polymerization, yielding polymers with improved properties. Nanofibrous polyethylene was also obtained under polymerization conditions with the use of this supported catalyst.

Keywords: SBA-15 zeolite; Zirconium catalyst; Heterogeneous catalysis; Ethylene polymerization; Nanofibrous polyethylene

1. Introduction

The synthesis of polymers with improved properties and controlled morphology is of great interest to both academia and industry. So far, most polymers have been produced by organometallic catalysts in the process of olefin polymerization [1–3]. These homogeneous catalysts, such as metallocene [4,5] and post-metallocene [6,7], have very high catalytic activity; however, the lack of control over the morphology of polymers limits their application. One way to solve this problem is to immobilize these catalysts on suitable supports [8,9]. Immobilization of homogeneous catalysts for olefin polymerization is accomplished by the process of supporting the transition-metal complexes and MAO on the surface of inorganic solids or polymers, causing the contributing part to be adsorbed. Since the supports can effectively control the structure and morphology of polymers through polymerization [10], the properties of the obtained polymers can be greatly improved. First used in the 1990s, mesoporous zeolite with a parallel hexagonal channel structure is becoming a promising support for catalyst immobilization [11–13]. The geometrical constraints of the parallel hexagonal channel structure affect the pattern of monomer insertion and the chain growth process, which offer a way to control the polymer chain structure and morphology in olefin polymerization [14,15]. Moreover, since the mesoporous zeolite has a nanoscale pore diameter, nanofibrous polymers can be obtained by olefin polymerization. A good example is provided by the work of Aida et al. [16], who produced the crystalline nanofibers of polyethylene with MSF-supported Cp_2TiCl_2 catalyst in the "extrusion polymerization."

In this work, we used SBA-15 as the support. As a mesoporous zeolite, SBA-15 has a lot of particular characteristics, such as large surface area, narrow pore distribution, long pore diameter, large pore volume, and high mechanical intensity sustained by a thick wall [17], so it is a very ideal support for homogeneous catalysts. Our group has reported the support of post-metallocene catalysts such as diimine nickel complex [18] and pyridine bisimine iron complex [19] on SBA-15, with some satisfying results. To develop this aspect of our research, we synthesized the zirconium catalyst bis[N-(3-*tert*-butylsalicylidene)-4′-allyloxylanilinato] zirco-

* Corresponding author. Fax: +86 21 65641740.
E-mail address: gxjin@fudan.edu.cn (G.-X. Jin).

0021-9517/$ – see front matter
doi:10.1016/j.jcat.2005.06.002

nium(IV) dichloride (Fig. 1) with very high catalytic activity, introduced it into the supported system, and characterized the property of polyethylene produced by the supported catalysts in the process of ethylene polymerization.

2. Experimental

2.1. Synthesis

All manipulations were performed under an argon atmosphere with standard Schlenk techniques. 3-*Tert*-butylsalicylaldehyde was prepared according to a method described in the literature [20]. 4-Acetamidophenol, $ZrCl_4$, and co-catalyst MAO (1.7 M in toluene) were purchased from the Acros and Witco Corporations, respectively; other reagents were analytical-grade reagents. Solvents were dried with anhydrous calcium dichloride or a 4-Å molecular sieve for several days, then refluxed with appropriate drying reagents (sodium/benzophenone for toluene, diethyl ether, hexane, THF, and CaH_2 for dichloromethane) and distilled under argon before use. As stated in Ref. [17], the synthesis of mesoporous zeolite SBA-15 included the use of triblock copolymer $EO_{20}PO_{70}EO_{20}$ (Pluronic P123, BASF) as the template and tetraethoxysilane (TEOS, 98%; Acros) as the source of silica.

2.2. Catalyst preparation

2.2.1. Preparation of homogenous catalyst bis[N-(3-tert-butylsalicylidene)-4′-allyloxylanilinato] zirconium(IV) dichloride (**2**) (Scheme 1)

*2.2.1.1. Synthesis of the ligand N-(3-tert-butylsalicylidene)-4′-allyloxylanilinato (**1**)* 4-Acetamidophenol (0.1 mol, 15.1 g), allylbromine (0.11 mol, 13.3 g), and potassium carbonate (0.25 mol, 34.6 g) were suspended in dried acetone, and the solution was refluxed for 24 h. After the solvent was cooled to room temperature, it was removed to give 13.1 g (69%) of 4-allyloxylacetylaniline. (^{1}H-NMR (500 MHz, $CDCl_3$): δ 2.12 (3H, s, acetyl), 4.49 (2H, d, CH_2), 5.26 (1H, d, $=CH_{cis}$), 5.40 (1H, d, $=CH_{trans}$), 6.02 (1H, m, –CH=), 6.83 (2H, d, phenyl), 7.36 (2H, d, phenyl), 7.58 (1H, s, –NHCO–).)

To a solution of 4-allyloxylacetylaniline (68 mmol, 13 g) in ethanol was added 136 mmol of hydrochloric acid (12 M, 11.3 ml), and the reaction mixture was refluxed for 6 h. After removal of solvent, the mixture was poured into NaOH solution and extracted with diethyl ether. The diethyl ether extract was dried over Na_2SO_4 and then concentrated to leave crude product. 4-Allyloxylaniline (7.6 g, 75%) was purified by distillation under vacuum. (^{1}H-NMR (500 MHz, $CDCl_3$): δ 3.32 (2H, s, NH_2), 4.43 (2H, d, CH_2), 5.24 (1H, d, $=CH_{cis}$), 5.38 (1H, d, $=CH_{trans}$), 6.01 (1H, m, –CH=), 6.59 (2H, d, phenyl), 6.73 (2H, d, phenyl).)

A solution of 4-allyloxylaniline (2.25 g, 15.1 mmol) in ethanol was added to a 3-Å molecular sieve (2 g) and 3-*tert*-butylsalicylaldehyde (2.39 g, 13.4 mmol) in ethanol drop by drop; then the reaction mixture was stirred for 24 h at room temperature. After filtration, ethyl acetate was used to wash the molecular sieve. The combined organic phases were evaporated in vacuo to give a crude product, which was purified by column chromatography on silica gel with hexane/ethyl acetate (10:1) as eluent to give the ligand **1** (3.4 g) as a pale yellow oil in 82% yield. (^{1}H-NMR

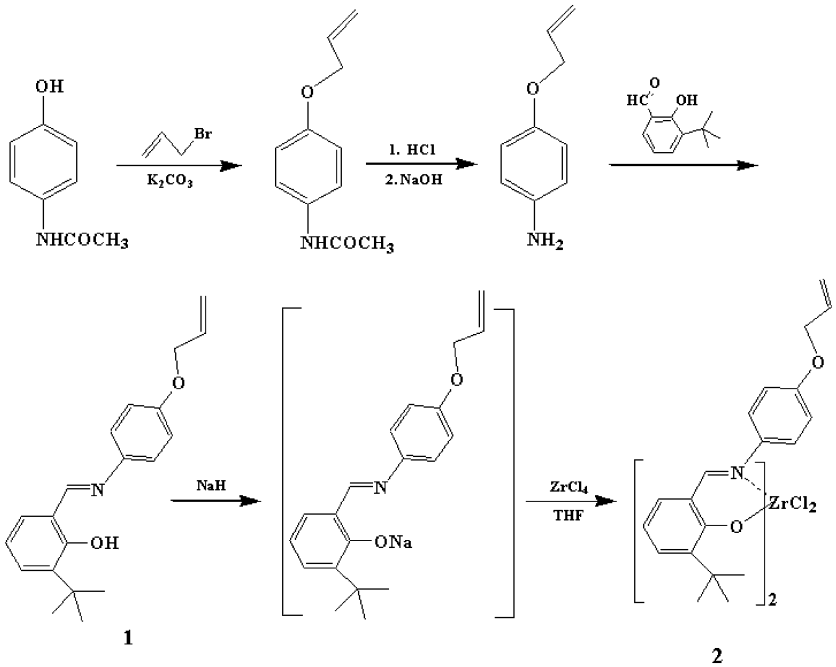

Scheme 1. Synthesis of complex **2**.

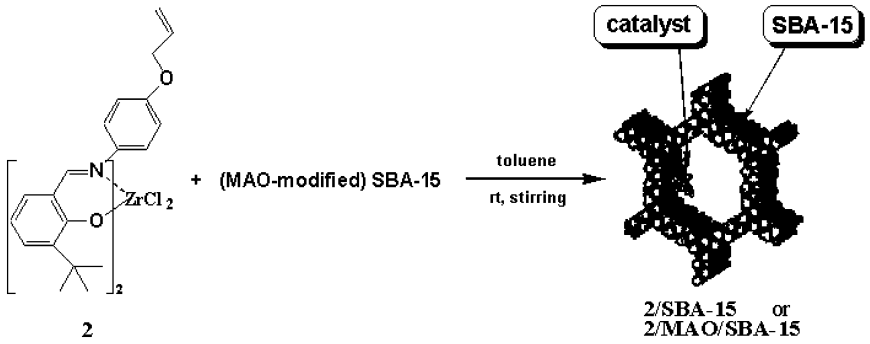

Scheme 2. The synthetic route of SBA-15 supported zirconium catalysts (**2**/SBA-15 and **2**/MAO/SBA-15).

(500 MHz, $CDCl_3$): δ 1.47 (9H, s, *tert*-butyl), 4.56 (2H, d, CH_2), 5.32 (1H, d, $=CH_{cis}$), 5.45 (1H, d, $=CH_{trans}$), 6.05 (1H, m, –CH=), 6.86 (1H, t, phenyl), 6.95 (2H, d, phenyl), 7.23–7.27 (3H, m, phenyl), 7.36 (1H, d, phenyl), 8.60 (1H, s, –CH=N), 14.03 (1H, s, OH).)

2.2.1.2. Synthesis of the catalyst (2) A solution of **1** (2.0 g, 6.5 mmol) in 50 ml THF was added drop by drop to NaH (60%, 0.86 g, 21.5 mmol). After 2 h of stirring, a solution of $ZrCl_4$ (0.72 g, 3.1 mmol) in 50 ml THF was added, and the reaction mixture was stirred for 24 h at room temperature. After removal of THF, CH_2Cl_2 was used for extraction and then concentrated. The crude product was recrystallized by CH_2Cl_2/hexane to give 1.49 g (62%) of complex **2**. (^{1}H-NMR (500 MHz, $CDCl_3$): δ 1.42 (18H, s, *tert*-butyl), 4.37 (4H, d, CH_2), 5.32 (4H, m, $=CH_2$), 6.04 (2H, m, –CH=), 6.57 (2H, d, phenyl), 6.90–7.42 (12H, m, phenyl), 8.07 (2H, s, –CH=N).)

2.2.2. Preparation of supported catalysts (2/SBA-15 and 2/MAO/SBA-15)

The SBA-15-supported zirconium catalysts were prepared by the method we have reported [18,19], as shown in Scheme 2. For **2**/SBA-15, 0.3 g of SBA-15 was heated at 200 °C under vacuum for 8 h. After the sample was cooled to room temperature, 20 ml of toluene was added. It was then directly mixed with 10 ml of toluene solution of 0.038 g complex **2**. After 20 h of stirring at room temperature, the supported catalyst was collected and washed five times with toluene and three times with hexane, and then dried under vacuum to give a light yellow powder. For **2**/MAO/SBA-15, 0.3 g of SBA-15 was heated at 200 °C under vacuum for 8 h. After the sample was cooled to room temperature, 20 ml of toluene was added. It was then mixed with 10 ml of toluene solution of 2 ml MAO, and the slurry was stirred for 20 h at room temperature and filtered. The MAO-modified SBA-15 was collected and washed five times with toluene and three times with hexane, and then dried under vacuum. Subsequently, 30 ml of toluene solution of 0.041 g complex **2** was added to the solid, the slurry was stirred for another 20 h at room temperature and filtered. The supported catalyst was collected and washed five times with toluene and three times with hexane, and then dried under vacuum to give an orange powder.

2.3. Ethylene polymerization

High-pressure ethylene polymerization with homogeneous and supported catalysts was carried out in a 200-ml autoclave stainless-steel reactor equipped with a mechanical stirrer and a temperature controller. Fifty milliliters of toluene and the desired amount of co-catalyst MAO were added in that order, and the mixture was stirred at 800 rpm for 10 min while being heated up to the reaction temperature. The catalyst solution or slurry was then added to the reactor, and ethylene with the desired pressure was introduced to start the polymerization. After 0.5 h, the polymerization was stopped by the addition of a 1 vol% HCl/ethanol solution, and the polyethylene was collected by filtration, thoroughly washed with ethanol, and dried at 40 °C under vacuum until constant weight.

2.4. Characterization of support, catalysts, and polymers

Suitable crystals for X-ray analysis of complex **2** were obtained by slow diffusion of hexane into CH_2Cl_2 solution of the corresponding compound. None showed signals of decomposition during X-ray data collection, which was carried out at room temperature. Details of the data collection and refinement are summarized in supplementary information. Selected bond lengths and angles are given in Fig. 1. Diffraction data were collected at 293 K on a Bruker Smart APEX CCD diffractometer (Mo-K_α radiation). The structure was determined by direct methods with SHELX-97 and refined by fullmatrix least-squares calculations, with the program system SHELXTL-97. Crystallographic data (excluding structure factors) for the structure reported in this paper have been deposited in the Cambridge Crystallographic Data Center (CCDC 209833) for complex **2**. (Copies of the data can be obtained free of charge by application to The Director, CCDC, 12 Union Road, Cambridge CB2 1EZ, UK (fax: +44 1223 336033; e-mail: deposit@ccdc.cam.ac.uk or www: http.ccdc.cam.ac.uk).)

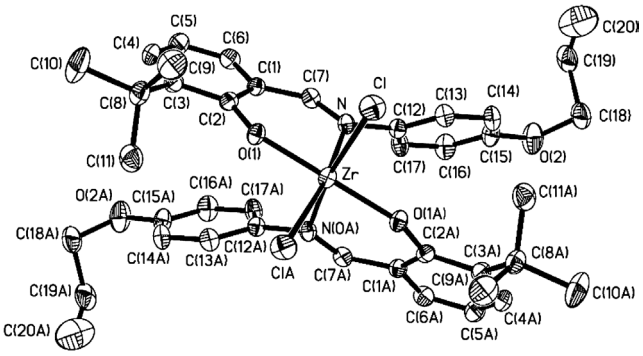

Fig. 1. The molecular structure of complex **2**. The hydrogen atoms are omitted for clarity. Selected distances (Å) and angles (°): Zr–O(1) = 1.9911(18), Zr–N = 2.354(2), Zr–Cl = 2.4237(9), O(1)–C(2) = 1.337(3), C(2)–C(1) = 1.402(4), C(1)–C(7) = 1.436(4), N–C(7) = 1.297(3), N–C(12) = 1.453(3), O(1)–Zr–O(1A) = 165.39(11), O(1)–Zr–Cl = 95.67(6), O(1)–Zr–N = 77.27(8), N–Zr–Cl = 94.14(7), O(1)–Zr–N = 90.97(8), Zr–O(1)–C(2) = 146.33(19), C(12)–N–Zr = 119.40(18), C(7)–N–Zr = 124.7(2).

The loading of zirconium and aluminum in the supported catalysts was determined by ICP-AES measurements. ^{1}H NMR spectra were recorded on a Bruker VAVCE-DMX 500 spectrometer in $CDCl_3$. X-ray diffraction (XRD) patterns were recorded with a Bruker D4 Endeavor diffractometer with Cu-K_α radiation (40 kV, 40 mA). The pore structure of the support was evaluated with TEM (JEM2011). Nitrogen adsorption–desorption isotherms were measured at 77 K with a Tristar 3000 volumetric adsorption apparatus from Micrometritics. The surface areas of the samples were obtained with a technique based on the standard BET method. The average pore diameter was calculated with the BJH method.

The molecular weight of the produced polyethylene was determined by intrinsic viscosity measurements in decahydronaphthalene (decalin) at 135 °C with an Ubbelohde viscometer by a one-point method [21] and calculated accordingly. The polymers were characterized with a Perkin–Elmer DSC 4 thermal analyzer with a heating rate of 10 °C/min in the range from 45 to 160 °C. Melting points (T_m) were related to the second heating process. SEM study of support and polyethylene morphology was carried out with a Philips XL30 device.

3. Results and discussion

In this study, we use the homogeneous catalyst–zirconium complex possessing two phenoxy-imine chelate ligands. A general synthetic route for this complex is shown in Scheme 1. This route uses materials that are easily prepared and relatively stable. The overall yield of all the steps is very good.

The ORTEP diagram of complex **2** is presented in Fig. 1. The molecular structure of complex **2** reveals that the two oxygen atoms occupy trans positions [O(1)–Zr–O(1A) angle, 165.4°], whereas the two nitrogen atoms and the two chlorine atoms are situated in cis positions [N–Zr–N(0A) angle, 73.7°; Cl–Zr–Cl(A) angle, 99.3°]. Therefore, complex **2** adopts a distorted octahedral structure around the zirconium center, which is similar to the structure of zirconium catalyst reported in the literature [7]. This demonstrates that the presence of oxygen atoms [Fig. 1, O(2) and O(2A)] does not break the structure of the active center, making complex **2** with high catalytic activity in polymerization (Table 1).

Mesoporous zeolite SBA-15 obtained by hydrothermal synthesis has a uniform hexagonal array of linear channels constructed with a honeycomb-like silica matrix [17]. The results of N_2 adsorption/desorption demonstrate that the BET surface area, pore volume, and average pore diameter of SBA-15 are about 528 m^2/g, 0.91 ml/g, and 7.15 nm, respectively. The SEM (a) and TEM (b) images of SBA-15 are shown in Fig. 2. After complex **2** is supported on MAO-modified SBA-15 (Scheme 2), all three parameters become smaller (335 m^2/g, 0.49 ml/g, 6.01 nm), confirming that the catalyst molecule is chemically adsorbed to the surface of the SBA-15 channel. The N_2 adsorption/desorption isotherms and pore size distribution curves in Fig. 3 clearly show the difference between **2**/MAO/SBA-15 and SBA-15. The larger pores of SBA-15 are filled at higher relative pressure, as represented in Fig. 3. Moreover, narrow pore size distribution is characteristic for both samples, but the peak value of **2**/MAO/SBA-15 (3.9 nm) is smaller than that of SBA-15 (7.9 nm).

The XRD pattern for SBA-15 shows three characteristic absorption peaks (Fig. 4) that are indexed as (100), (110),

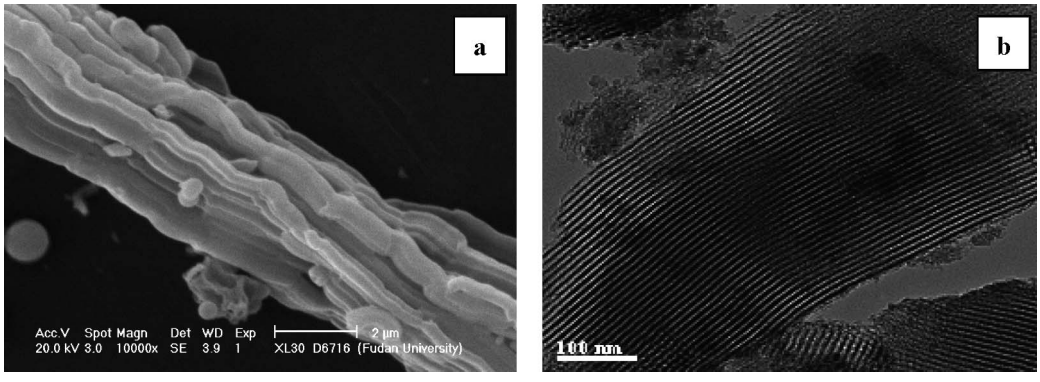

Fig. 2. SEM and TEM images of mesoporous zeolite SBA-15.

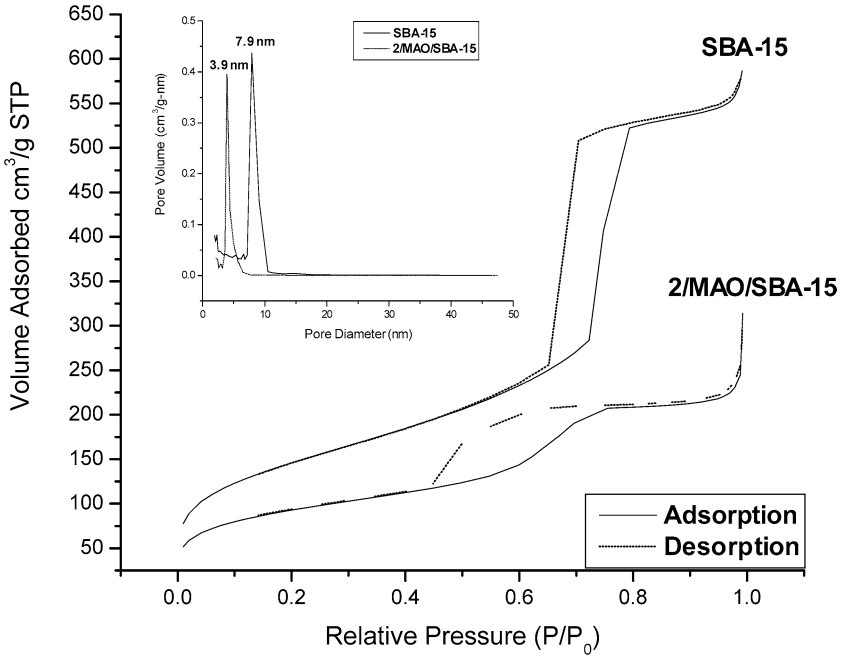

Fig. 3. The N_2 adsorption/desorption isotherms and pore size distribution curves for **2**/MAO/SBA-15 and SBA-15.

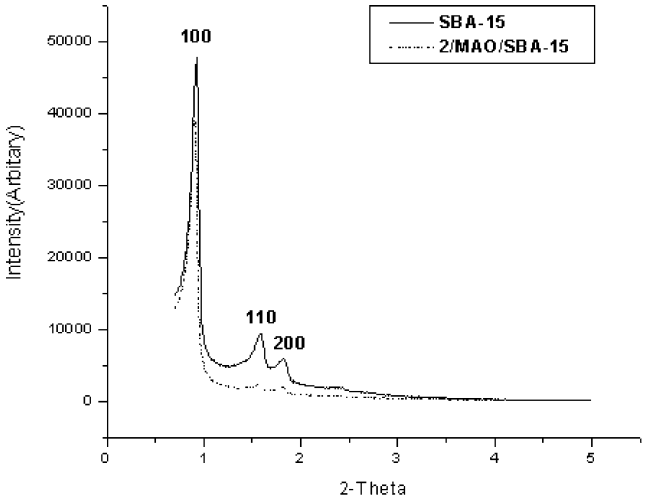

Fig. 4. The XRD patterns for **2**/MAO/SBA-15 and SBA-15.

(200). For **2**/MAO/SBA-15, the XRD pattern shows that the three peaks still exist, and the peak positions do not change. Furthermore, since the two samples are measured under the same conditions, the reduced intensity for the **2**/MAO/SBA-15 can be explained by the existence of complex **2** and MAO in the channel of the support. This phenomenon demonstrates that the two-dimensional ordered channel structure of the support is not destroyed in the process of immobilization; this is very important for controlling the morphology and dimensions of polymers in polymerization.

The results obtained in ethylene polymerization are shown in Table 1. Compared with the homogeneous catalyst, a decrease in catalytic activity is observed in the supported system. Directly support of complex **2** on SBA-15 results in no catalytic activity. On the other hand, the supported catalyst still has fairly high activity when MAO modifies the mesoporous zeolite. Fig. 5 shows plausible models on the surface species in the supported system. Directly supported on SBA-15 that is silica, complex **2** is believed to be anchored through the formation of a μ–oxo-like bond with a hydroxyl group of support [14], as presented in Fig. 5a. For MAO-modified support, however, the cationic species L_2Zr^+Cl are trapped and stabilized by multicoordinating oligomeric MAO complexes [22], as represented by Fig. 5b.

Table 1
The results of ethylene polymerization with supported and homogeneous zirconium catalysts

Catalyst	$Zr_{anal.}$ (wt%)	$Al_{anal.}$ (wt%)	m_{cat} (mg)	Yield (g)	Activity[a]	T_m (°C)	Mv[b]
2/SBA-15	1.28	–	7.1	trace	–	–	–
2/MAO/SBA-15	0.85	20.6	10.7	1.5	3.0	138.9	1,400,000
2	–	–	0.8	5.4	10.8	129.8	400,000

Note. Co-catalyst: MAO. Polymerization conditions: 50 ml of toluene, $n(Zr) = 1.0$ μmol, ethylene pressure = 10 atm, temperature = 40 °C, time = 30 min and total aluminoxane to Zr ratio = 3000.

[a] Activity unit: 10^6 $g_{PE}/(mol_{Zr}\ h)$.

[b] Viscosity average molecular weight.

Table 2
The results of ethylene polymerization over **2**/MAO/SBA-15 under different conditions

Run	Al/Zr[a]	Ethylene pressure (atm)	Temperature (°C)	Yield (g)	Activity (10^6 $g_{PE}/(mol_{Zr}\,h)$)	T_m (°C)	Mv[b]
1	3000	10	40	1.5	3.0	138.9	1,400,000
2	2000	10	40	2.5	5.0	137.0	730,000
3	4000	10	40	2.6	5.2	137.4	540,000
4	3000	10	20	0.7	1.4	136.9	870,000
5	3000	10	60	3.1	6.2	136.4	10,000
6	3000	7	40	1.7	3.4	136.9	1,400,000
7	3000	4	40	0.5	1.0	137.1	28,000

Note. Co-catalyst: MAO. Polymerization conditions: 50 ml of toluene, $n(Zr) = 1.0$ μmol and time = 30 min.
[a] Total aluminoxane to Zr ratio.
[b] Viscosity average molecular weight.

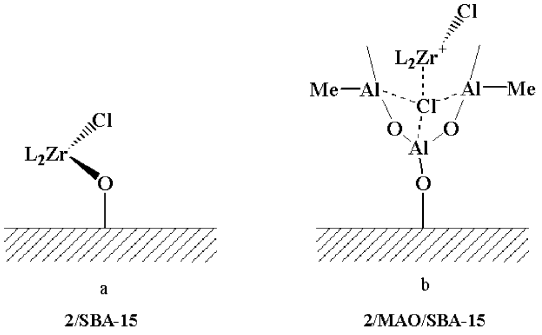

Fig. 5. Surface species models of various zirconium catalysts supported on SBA-15 [L = N-(3-*tert*-butylsalicylidene)-4′-allyloxylanilinato].

Since the active centers in the catalyst system for polymerization are the cationic species L_2Zr^+Cl, both models could explain why the zirconium catalysts supported directly on SBA-15 are not active in ethylene polymerization whereas those supported on MAO-modified SBA-15 are active.

Table 1 also shows that the molecular weight of the polyethylene obtained with **2**/MAO/SBA-15 is more than three times higher than that obtained with the homogeneous catalyst. This increase in molecular weight of the polymers indicates that the support is very efficient in reducing chain transfer reactions during polymerization. This can be explained by a large steric hindrance of the active centers influenced by the channel walls, thus inhibiting the occurrence of β-H elimination in polymer growth and slowing down the chain transfer rate. The melting point of polyethylene produced by **2**/MAO/SBA-15 is much higher than that produced by its homogeneous counterpart; this can be explained by the higher crystallinity and higher molecular weight of the polymer obtained with **2**/MAO/SBA-15. The high melting point (138.9 °C) indicates the formation of linear high-density polyethylene [11].

The results for ethylene polymerization catalyzed by **2**/MAO/SBA-15 are collected in Table 2. Under various conditions, the supported catalyst **2**/MAO/SBA-15 has a high activity (10^6 $g_{PE}/(mol_{Zr}\,h)$), and the molecular weight of the obtained polymers is much higher (except Runs 5 and 7). In addition, it is revealed that the catalytic activity is dependent upon the Al/Zr molar ratio (Table 2, Runs 1–3). At a ratio of 3000, the activity is at its lowest point, but the intrinsic viscosity molecular weight Mv of the obtained polymers is the highest. The activity of **2**/MAO/SBA-15 increases when the temperature of polymerization rises from 20 to 60 °C (Table 2, Runs 1, 4, and 5), because the concentration of the active center activated by MAO increases as the temperature rises [23]. Furthermore, an increase in temperature results in the reduction of molecular weight due to the great increase in the rate of chain transfer. It is clear that both the activity of **2**/MAO/SBA-15 and the molecular weight of the obtained polymers decrease markedly at low ethylene pressure (Table 2, Run 7), indicating that this supported catalyst would only be valuable at high ethylene pressure ($\geqslant$7 atm). Moreover, all of the polymers have high melting points ($\sim$137 °C), confirming that the SBA-15-supported catalyst can produce polyethylene with an extended chain structure and high crystallinity.

Fig. 6 shows the micrographs of polyethylene produced by **2**/MAO/SBA-15 and complex **2** with different magnifications. Inspection of the micrographs reveals striking differences among the polymers. Figs. 6a and 6b reveal discrete, ultrathin polyethylene fibers about 60 nm in diameter, which suggests that the two-dimensional ordered channel structure of SBA-15 can undoubtedly control the relative position between the polymer chains. Fig. 6c shows the bundles of polyethylene fibers at small magnification. When the magnification becomes even smaller (Figs. 6d and 6e), lots of nanofibers aggregate loosely to form fiber aggregates. This demonstrates that the nanofibrous morphology is representative of the total polymers formed in the "extrusion polymerization." The morphology of these polymers is quite different from the sheet structure of polyethylene produced by complex **2**, as shown in Fig. 6f. In the supported catalyst system, polymers grow with the template of SBA-15, and the nanopore diameter of SBA-15 can effectively confine the direction and dimension of olefin polymerization, which indicates the good potential of using mesoporous zeolite for the control of polymer chain structure and morphology.

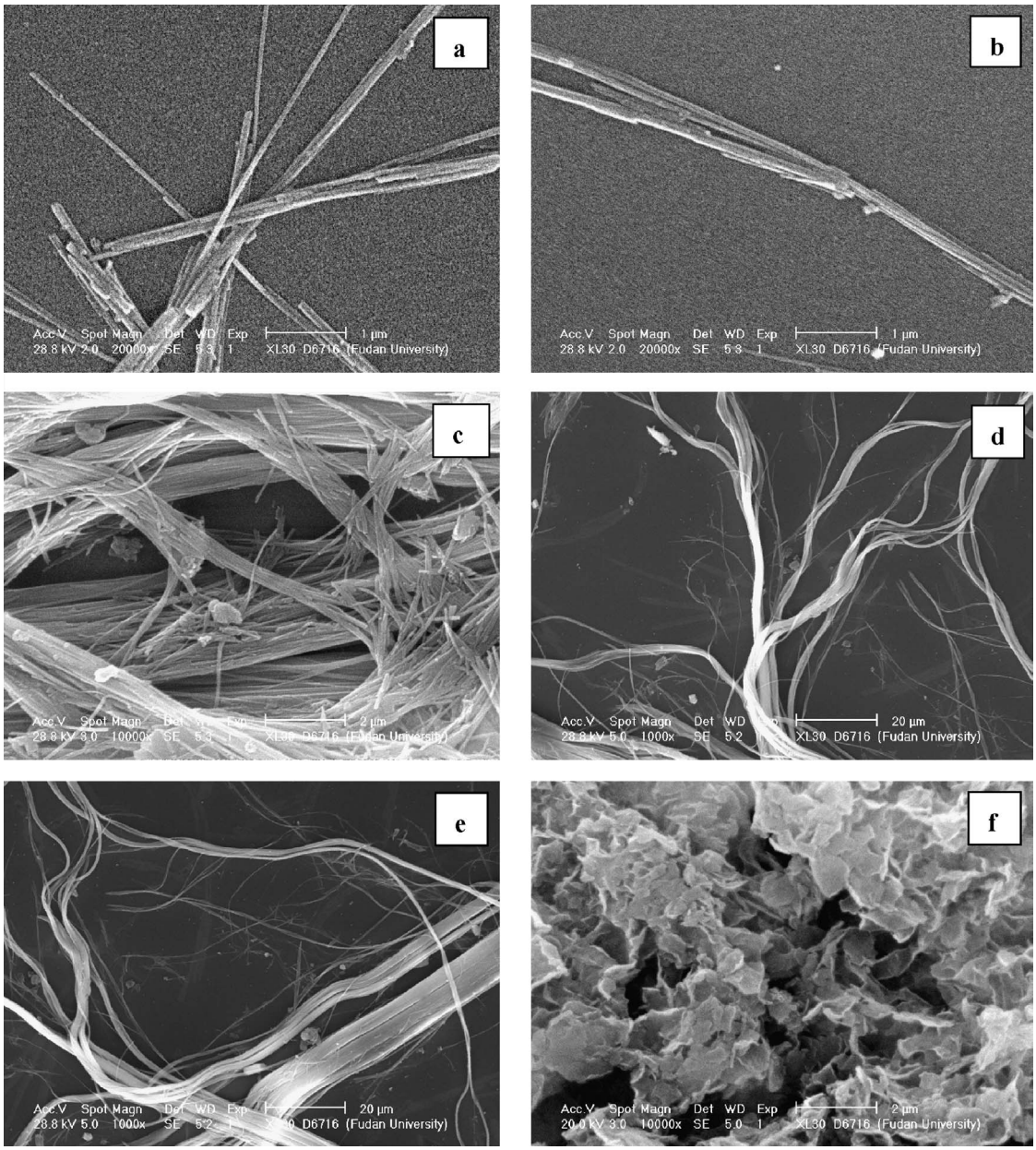

Fig. 6. SEM images of polyethylene produced by **2**/MAO/SBA-15 (a)–(e) and **2** (f).

4. Conclusions

The mesoporous zeolite SBA-15 was an ideal support for immobilizing homogeneous catalysts for olefin polymerization. As a good example, we used the very active zirconium catalyst-bis[N-(3-*tert*-buttylsalicylidene)-4′-allyloxylanilinato] zirconium(IV) dichloride in the supported catalyst system. Directly support of the homogeneous catalyst on SBA-15 showed no activity, but the supported catalyst had fairly high activity when MAO was used to modify SBA-15. In polymerization, the supported catalyst successfully controlled the morphology of polyethylene and produced nanofibrous polymers. Both the molecular weight and melting point of this nanofibrous polyethylene were much higher; these polymers have a great potential for application.

Acknowledgments

Financial support by the National Nature Science Foundation of China for Distinguished Young Scholar (29925101, 20421303) and by the Special Funds for Major State Basic Research Projects (Grant No. 1999064800) is gratefully acknowledged.

Supplementary information

Supplementary information for this article may be found on ScienceDirect, in the online version.

Please visit DOI: 10.1016/j.jcat.2005.06.002.

References

[1] A. Zambelli, A. Ammendola, A. Grassi, P. Longo, A. Proto, Macromolecules 19 (1986) 2703.
[2] M. Avella, E. Martuscelli, G. Volpe, A. Segre, E. Rozzi, T. Simonazi, Macromol. Chem. 187 (1986) 1927.
[3] G.W. Coates, R. Waymouth, J. Am. Chem. Soc. 115 (1993) 91.
[4] H. Sinn, W. Kaminsky, Adv. Organomet. Chem. 18 (1980) 99.
[5] W. Kaminsky, M. Arndt, Adv. Polym. Sci. 127 (1997) 143.
[6] B.L. Small, M. Brookhart, J. Am. Chem. Soc. 120 (1998) 7143.
[7] S. Matsui, M. Mitani, J. Saito, Y. Tohi, H. Makio, N. Matsukawa, Y. Takagi, K. Tsuru, M. Nitabaru, T. Nakano, H. Tanaka, N. Kashiwa, T. Fujita, J. Am. Chem. Soc. 123 (2001) 6847.
[8] G.G. Hlatky, Chem. Rev. 100 (2000) 1347.
[9] (a) C. Liu, G.-X. Jin, New J. Chem. (2002) 1485;
(b) D. Zhang, G.-X. Jin, N. Hu, Chem. Commun. (2002) 574;
(c) D. Zhang, G.-X. Jin, Organometallics 22 (2003) 2851.
[10] K. Tajima, T. Aida, Chem. Commun. (2000) 2399.
[11] H. Rahiala, I. Beurroles, T. Eklund, K. Hakala, R. Gougeon, P. Trens, J.B. Rosenholm, J. Catal. 188 (1999) 14.
[12] M. Risch, E.E. Wolf, Appl. Catal. A: Gen. 206 (2001) 283.
[13] C. Song, R.K. Madhusudan, Appl. Catal. A: Gen. 176 (1999) 1.
[14] K.S. Lee, C.G. Oh, J.H. Yim, S.K. Ihm, J. Mol. Catal. A: Chem. 159 (2000) 301.
[15] Z. Ye, H. Alsyouri, S. Zhu, Y.S. Lin, Polymer 44 (2003) 969.
[16] K. Kageyama, J. Tamazawa, T. Aida, Science 285 (1999) 2113.
[17] D. Zhao, J. Feng, Q. Huo, N. Melosh, G.H. Fredrickson, B.F. Chmelka, G.D. Stucky, Science 279 (1998) 548.
[18] C. Guo, D. Zhang, G.-X. Jin, Chinese Sci. Bull. 49 (2004) 249.
[19] C. Guo, G.-X. Jin, F. Wang, J. Polym. Sci. A: Polym. Chem. 42 (2004) 4830.
[20] G. Casiraghi, G. Casnati, G. Puglia, G. Sartori, G. Terenghi, J. Chem. Soc., Perkin Trans. I (1980) 1862.
[21] J.H. Elliott, K.H. Horowitz, T. Hoddock, J. Appl. Polym. Sci. 19 (1970) 2947.
[22] J.C.W. Chien, D. He, J. Polym. Sci. A: Polym. Chem. 29 (1991) 1603.
[23] X. Wang, G.-X. Jin, Organometallics 23 (2004) 6319.